

$B^3\Sigma_u^- - X^3\Sigma_g^-$  transition in selenium dimer: *ab initio* multireference configuration interaction calculations

This article has been downloaded from IOPscience. Please scroll down to see the full text article.

2011 Chinese Phys. B 20 043101

(<http://iopscience.iop.org/1674-1056/20/4/043101>)

View [the table of contents for this issue](#), or go to the [journal homepage](#) for more

Download details:

IP Address: 159.226.165.151

The article was downloaded on 16/10/2012 at 07:33

Please note that [terms and conditions apply](#).

# $B^3\Sigma_u^- - X^3\Sigma_g^-$ transition in selenium dimer: *ab initio* multireference configuration interaction calculations\*

Yan Bing(闫冰)<sup>a)†</sup>, Liu Li-Li(刘立莉)<sup>a)</sup>, Wei Chang-Li(魏长立)<sup>a)</sup>,  
Guo Jing(郭晶)<sup>a)</sup>, and Zhang Yu-Juan(张玉娟)<sup>b)</sup>

<sup>a)</sup>*Institute of Atomic and Molecular Physics, Jilin University, Changchun 130012, China*

<sup>b)</sup>*Changchun Institute of Optics, Fine Mechanics and Physics, Chinese Academy of Sciences, Changchun 130033, China*

(Received 6 July 2010; revised manuscript received 4 January 2011)

Theoretical investigation of low-lying electronic states and  $B^3\Sigma_u^- - X^3\Sigma_g^-$  transition properties of selenium dimer using size-extensivity singly and doubly excitation multireference configuration interaction theory with nonrelativistic all-electron basis set and relativistic effective core potential plus its split valence basis set is presented in this paper. The spectroscopic constants of ten low-lying  $A-S$  bound states have been obtained and compared with experiments. Spin-orbit calculations for coupling between  $B^3\Sigma_u^-$  states and repulsive  $^1\Pi_u$ ,  $^5\Pi_u$  states have been made to interpret the predissociation mechanisms of the  $B^3\Sigma_u^-$  state. The lifetimes of  $B^3\Sigma_u^-$  ( $\nu = 0 \sim 6$ ) have been calculated with scalar relativistic effects included or excluded, respectively, and reasonably agree with experimental values.

**Keywords:** potential energy curve, lifetime, spin-orbit coupling, selenium dimer

**PACS:** 31.15.ae, 31.15.aj, 31.15.ag, 31.15.Df

**DOI:** 10.1088/1674-1056/20/4/043101

## 1. Introduction

Early in the 1970s, lasing was achieved by pumped group VI dimers, such as  $S_2$ ,  $Se_2$ , and  $Te_2$ .<sup>[1]</sup> The transition from selected vibrational-rotational levels of  $B^3\Sigma_u^-$  state to higher levels of ground state  $X^3\Sigma_g^-$  leads to continuous radiation in lasing. The electronic structure and spectroscopy of group VI dimers have attracted much theoretical and experimental interest in previous investigations for their applications in laser techniques,<sup>[2-4]</sup> especially for the dipole allowed  $B-X$  band. The  $B-X$  transition of  $S_2$  molecule, which is widely used for the tunable laser in ultraviolet and visible regions of spectrum and radio-frequency sulfur lamp,<sup>[5]</sup> is thoroughly investigated, while for the heavier dimers  $Se_2$  and  $Te_2$  the information about electronic structure and spectroscopy is not very extensive.

Early spectroscopic measurement results have been compiled by Hertzberg.<sup>[6]</sup> In 1982, Prosser and co-workers recorded laser-excited fluorescence of gaseous  $Se_2$  molecules by Fourier transform spectrometry and determined the spectroscopic constants of  $X$  and  $B$  states of  $Se_2$ .<sup>[7]</sup> Recently, the emis-

sion band of magnetic dipole transition  $a^1\Delta_g - X^3\Sigma_g^-$  was also observed and the  $a^1\Delta_g$  was characterized experimentally.<sup>[8]</sup> The early experimental results for radiative lifetime of  $B$  state of  $Se_2$  molecule,  $(85 \pm 5)$  ns<sup>[9]</sup> by fitting  $A$  and  $B$  state fluorescence,  $(39 \pm 5)$  ns<sup>[10]</sup> for  $\nu = 0$ ,  $J = 129$  level, and  $(58 \pm 6)$  ns<sup>[11]</sup> for  $\nu = 0$ ,  $J = 105$  level, differ greatly from each other. The latest experiment reported the collision-free rovibrational resolved fluorescence lifetimes of the  $B$  state of  $^{80}Se_2$ ,  $(47 \pm 4)$  ns for the  $\nu = 3 \sim 6$ ,  $J < 82$  unperturbed levels.<sup>[12]</sup>

The electronic structure and transition of the selenium dimer have previously been the subject of theoretical interest. Bhanuprakash *et al.* calculated the lifetimes of  $a^1\Delta_g$  and  $b^1\Sigma_g^+$  states by multireference configuration interaction (MRCI) method.<sup>[13]</sup> A systematic *ab initio* molecular orbital calculation on the  $Se_2$  molecule was performed in 1996,<sup>[14]</sup> the ground- and excited-state properties of neutral and anionic selenium dimers were investigated, and the radiative lifetime of  $B^3\Sigma_u^-$  state was evaluated as 61 ns with  $\pm 50\%$  uncertainty. The spin-mixed potential energy curves of ground and excited states of  $Se_2$  and  $Se_2^+$  molecules were calculated by spin-

\*Project supported by the National Natural Science Foundation of China (Grant No. 10604022), Chinese National Fusion Project for ITER (Grant No. 2010GB104003) and the Fundamental Research Funds for the Central Universities (Grant No. 200903369).

†Corresponding author. E-mail: yanbing@jlu.edu.cn

© 2011 Chinese Physical Society and IOP Publishing Ltd

<http://www.iop.org/journals/cpb> <http://cpb.iphy.ac.cn>

orbit multiconfigurational quasidegenerate perturbation (SO-MCQDPT) theory to interpret the ionization spectrum of  $\text{Se}_2$  molecule.<sup>[15]</sup> The present calculations aim at spontaneous lifetimes of vibrational levels of  $B^3\Sigma_u^-$  state of  $^{80}\text{Se}_2$  molecule using nonrelativistic and relativistic multireference configuration interaction methods with single and double excitations and Davison size-extensivity correction (MRCI(SD)+Q). According to our best knowledge, no previous calculations exist for lifetimes of vibrational levels of  $\text{Se}_2$  ( $B^3\Sigma_u^-$ ). Since the same theoretical strategies have been used to predict the transition properties of second-row dimer and good agreement with experiments has been reached in our previous study,<sup>[16]</sup> only a short description for the theoretical strategies is presented in this paper. Firstly two sets of potential energy curves (PEC) for  $B$  and  $X$  states, including and excluding the relativistic effect, of  $A-S$  states of  $\text{Se}_2$  were constructed. Then, on the basis of constructed PEC, accompanied by the calculated transition dipole moment function, the spontaneous lifetimes of vibrational levels of  $\text{Se}_2$  ( $B^3\Sigma_u^-$ ) were calculated. Some other low-lying spin-free electronic states were also investigated by MRCI(SD)+Q methods with scalar relativistic effects included, and the corresponding spectroscopic constants were fitted for comparison. The predissociation mechanisms of the  $B^3\Sigma_u^-$  state are also discussed based on *ab initio* spin-orbit coupling calculations.

## 2. Methods and computational details

Two sets of MRCI(SD)+Q calculations, that is nonrelativistic calculations with all-electron (AE) correlation-consistent polarized valence quadruple zeta (cc-pvQz)<sup>[17]</sup> basis set and scalar relativistic calculations with relativistic effective core potential (RECP) basis set, in which the mass-velocity and Darwin effects are considered, were performed separately to construct the adiabatic PECs of  $B^3\Sigma_u^-$  and  $X^3\Sigma_g^-$  states of  $\text{Se}_2$  molecule. The RECP ECP10MDF basis set for [Ne] core of Se atom combined with its split valence basis set aug-cc-pvQz<sup>[18]</sup> was used in RECP calculations. The restricted Hartree-Fock wavefunctions were obtained as the initial guess for completed active space multiconfiguration self-consistent field (CAS-MCSCF) calculations at different given internuclear distances from 0.15 nm to 0.6 nm. The active space comprises 12 valence electrons in 8 valence orbitals, and states that the aver-

age methodology was followed in MCSCF calculations. The dynamical correlation was obtained by single and double excitations out of CASSCF space, using an internal contraction MRCI(ic-MRCI) scheme as implemented in the Molpro package.<sup>[19]</sup> The PECs of other low-lying electronic states except for  $B$  and  $X$  were calculated by ic-MRCI+Q with RECP basis in the present work.

The spin-orbit coupling (SOC) correction was evaluated following the scalar relativistic calculations. The spin-orbit pseudopotentials were used for spin-orbit matrix elements and eigenstates by employing the state-interacting method, and the diagonal matrix elements of the perturbed Hamiltonian eigenmatrix were replaced by corresponding ic-MRCI+Q energies.

The radiative lifetime  $\tau_{v'}$  is defined by

$$\tau_{v'} = \left( \sum_{v''} A_{v'v''} \right)^{-1}, \quad (1)$$

where the Einstein coefficients  $A_{v'v''}$  represent the emission transition probabilities from upper vibrational levels  $v'$  to the lower ones  $v''$ . The Fermi golden rule treatment yields a conversion from dipole transition moment to Einstein coefficient,

$$A_{v'v''} (s^{-1}) = 2.026 \times 10^{-6} \tilde{\nu}^3 |\langle v' | R_e(r) | v'' \rangle|^2, \quad (2)$$

where  $\tilde{\nu}$  is the transition energy in unit  $\text{cm}^{-1}$ , and  $|\langle v' | R_e(r) | v'' \rangle|$  is the vibrational averaged transition moment in atomic units.

## 3. Results and discussion

### 3.1. PECs of $\text{Se}_2$

From 46 points calculated with the ic-MRCI+Q method for each electronic state, the 12 adiabatic PECs of  $\text{Se}_2$  molecule were constructed. As shown in Fig. 1, nine low-lying bound states correlating to the first three atom asymptotes  $\text{Se}(^3\text{P}) + \text{Se}(^3\text{P})$ ,  $\text{Se}(^3\text{P}) + \text{Se}(^1\text{D})$ , and  $\text{Se}(^3\text{P}) + \text{Se}(^1\text{S})$  are presented. In addition to these electronic states, the semi-bound  $^3\Pi_g$  state and repulsive  $^1\Pi_u$  and  $^5\Pi_u$  states, which cross with the  $B^3\Sigma_u^-$  state, were also calculated.

Table 1 collects the relative energy  $T_e$  of different electronic excited states at equilibrium geometries and potential parameters including optimized bond distances  $r_e$ , harmonic frequencies  $\omega_e$ , anharmonic frequencies  $\omega_e x_e$ , and rotation constants  $B_e$  for all bound states. A comparison is made against the values calculated by Heinemann *et al.*<sup>[14]</sup> and available experimental values.<sup>[7,8]</sup> The electronic ground state  $X^3\Sigma_g^-$

arises from the  $4p^4$  valence electrons of two Se atoms, and is dominant by  $8\sigma_g^2 4\pi_u^4 4\pi_g^2 8\sigma_u^0$  configuration (84% at internuclear distance  $R = 1.8 \text{ \AA}$ ,  $1 \text{ \AA} = 0.1 \text{ nm}$ ), while at large internuclear distance the ground state exhibits multireference characters. For example, the contribution of  $8\sigma_g^2 4\pi_u^4 4\pi_g^2 8\sigma_u^0$  configuration decreases rapidly to 62% at  $R = 3.0 \text{ \AA}$ . The multireference wavefunction descriptions are necessary for the configuration admixture of the  $\text{Se}_2$  electronic states. Compared with the most recent experiments, the RECP calculated bond distance of the  $X^3\Sigma_g^-$  state is  $\sim 0.01 \text{ \AA}$  larger, which is better than that from AE calculations for the inclusions of the scalar relativistic effect, the calculated  $\omega_e$  is  $\sim 4 \text{ cm}^{-1}$  smaller and  $\omega_e x_e$  is only  $\sim 0.4 \text{ cm}^{-1}$  smaller. The errors arise from finite basis sets (especially high polarized angular momentum functions) and the frozen core approximations, which

lead to partial correlation effects being neglected in calculations.

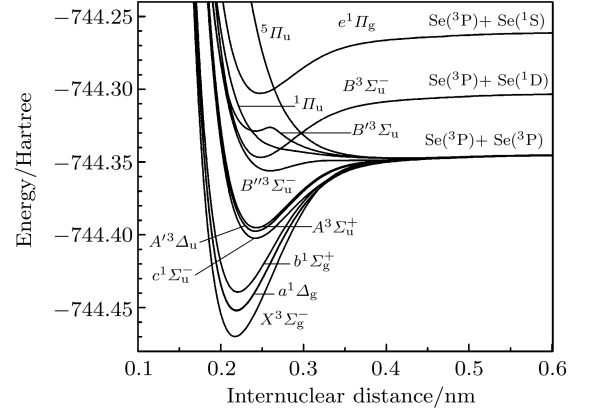


**Fig. 1.** Calculated potential energy curves of  $\text{Se}_2$  with MRCI(SD)+Q/RECP. 1 Hartree = 2 Ry = 27.21 eV.

**Table 1.** Relative energy ( $T_e$ ) and potential parameters of 10 electronic states from MRCI(SD)+Q/RECP calculations. The values in italics are from MRCI(SD)+Q/AE calculations of the present work. The values in square brackets are those calculated by Heinemann *et al.* in Ref. [14]. The values in parentheses are from experiments.

$A-S$ state	$r_e/\text{\AA}$	$\omega_e/\text{cm}^{-1}$	$\omega_e x_e/\text{cm}^{-1}$	$10^3 B_e/\text{cm}^{-1}$	$T_e/\text{cm}^{-1}$
$X^3\Sigma_g^-$	2.173	383.2	0.93	89.4	0
	2.188	382.9	0.95	88.1	0
	[2.181]	[386]	[1.04]	[88.6]	0
	(2.164) <sup>a</sup>	(387) <sup>a</sup>	(0.97) <sup>a</sup>	(90.1) <sup>a</sup>	0
$a^1\Delta_g$	2.190	364.7	0.98	88.0	3875
	[2.197]	[366]	[1.02]	[87.4]	[4618]
	(2.1767) <sup>b</sup>	(371.6) <sup>b</sup>	(1.02) <sup>b</sup>	(90.1) <sup>b</sup>	(4304) <sup>b</sup>
$b^1\Sigma_g^+$	2.2081	346.7	1.01	86.5	6701
	[2.218]	[345]	[1.16]	[85.7]	[7934]
	(2.193) <sup>a</sup>	(355) <sup>a</sup>	(1.10) <sup>a</sup>	(87.7) <sup>a</sup>	(7957) <sup>a</sup>
$c^1\Sigma_u^+$	2.417	272.0	1.33	72.2	14808
$A'^3\Delta_u$	2.418	273.4	1.29	72.1	15857
$A^3\Sigma_u^+$	2.426	269.2	1.26	71.7	16392
$B''^3\Pi_u$	2.592	177.7	3.67	6.26	24994
	[2.564]	[193]	[2.50]	[64.3]	[23829]
	(2.528) <sup>a</sup>	(191) <sup>a</sup>	(2.23) <sup>a</sup>	(66.0) <sup>a</sup>	(24158) <sup>a</sup>
$B^3\Sigma_u^-$	2.478	230.4	0.84	68.6	27006
	2.468	242.7	1.00	69.3	25506
	[2.448]	[252]	[1.06]	[70.5]	[24822]
	(2.443) <sup>a</sup>	(246) <sup>a</sup>	(1.17) <sup>a</sup>	(70.8) <sup>a</sup>	(25980) <sup>a</sup>
$B'^3\Pi_g$	2.413	228.2	2.33	72.5	30976
$e^1\Pi_g$	2.473	231.3	0.93	68.9	36641

<sup>a</sup> Experimental values from Ref. [7]; <sup>b</sup> Experimental values of  $a^1\Delta_g(a_2g)$  from Ref. [8].

The electronic transition from the  $4\pi_u$  orbital to  $4\pi_g$  gives rise to the  $8\sigma_g^2 4\pi_u^3 4\pi_g^3 8\sigma_u^0 B^3\Sigma_u^-$  state. The calculated equilibrium bond length of the  $B^3\Sigma_u^-$  state is 2.478 (RECP) or 2.468 (AE). Both values are  $0.02 \text{ \AA} \sim 0.03 \text{ \AA}$  larger than the experimental results. The relative larger deviation is due to the

exclusion of the 3d electron correlations of the Se atom in the present work, the correlations for  $n = 3$  shells are more important for the excited state calculations. The calculated  $\omega_e$  and  $\omega_e x_e$  are 230.4(242.7) and  $0.84(1.00) \text{ cm}^{-1}$ , which are in reasonable agreement with experiment. The  $T_e$  of  $B^3\Sigma_u^-$ ,  $27006 \text{ cm}^{-1}$

(RECP) or  $25506 \text{ cm}^{-1}$  (AE), is 3.9% or 1.8% higher than  $25980 \text{ cm}^{-1}$  in experiment, and close to the theoretical value  $24822 \text{ cm}^{-1}$ . Since the Einstein coefficient  $A$  is proportional to the cube of the excitation energy, the error of the excitation energy would lead 10% or 5% error for Einstein coefficient. The  $c^1\Sigma_u^+$ ,  $A'^3\Delta_u$ ,  $A^3\Sigma_u^+$ ,  $B'^3\Pi_g$ ,  $e^1\Pi_g$  states are firstly calculated and characterized in this work awaiting experimental results. The spectroscopic constants of the  $a^1\Delta_g$ ,  $b^1\Sigma_g^+$  and  $B''^3\Pi_u$  states were calculated and are listed in Table 1 with other experimental and theoretical results. The above states of less importance than  $B-X$  transitions are not discussed in detail in the present paper.

In Table 2, the spectroscopic constants of spin-

mixed curves for ground state  $X^3\Sigma_g^-$  are listed, from which little difference between  $\Omega = 1$  and  $\Omega = 0$  components is found. The bond distance difference is  $\sim 0.001 \text{ \AA}$ , the difference in harmonic frequency is  $\sim 2 \text{ cm}^{-1}$  and agrees with the experimental result  $1.7 \text{ cm}^{-1}$ . The calculated spin-orbit constant of the  $X$  state is  $482 \text{ cm}^{-1}$ ,  $\sim 6\%$  ( $\text{cm}^{-1}$ ) smaller than the experimental value. The error of spin-orbit constant is due to the pure Russell-Saunders ( $LS$ ) coupling scheme used for the high- $Z$   $\text{Se}_2$  system in the present calculations. The spin-orbit constant of the  $X$  state gives a 1.8% contribution to the  $B-X$  relative energy calculation, and leads to larger Einstein coefficients in lifetime calculations.

**Table 2.** Spectroscopic constants and spin-orbit constant for  $X^3\Sigma_g^-$  state from spin-orbit MRCI (SD) +Q/RECP calculations.

$\Omega$ state	$r_e/\text{\AA}$	$\omega_e/\text{cm}^{-1}$	$\omega_e x_e/\text{cm}^{-1}$	$10^3 B_e/\text{cm}^{-1}$	$T_e/\text{cm}^{-1}$
$X 0_g^+$	2.174	381.2	0.94	89.2	0
	–	(385.4) <sup>a</sup>	(0.98) <sup>a</sup>	(89.9) <sup>a</sup>	0
$X 1_g$	2.173	383.2	0.92	89.4	481.7
	–	(387.1) <sup>a</sup>	(0.96) <sup>a</sup>	(90.0) <sup>a</sup>	(511.9) <sup>a</sup>

<sup>a</sup> Experimental values from Ref. [7]

### 3.2. Predissociation of $\text{Se}_2$ ( $B^3\Sigma_u^-$ )

As illustrated in Fig. 1, the PEC of the  $B^3\Sigma_u^-$  state crosses with those of other spin-free states, including singlet  $\Pi_u$ , triplet  $\Pi_g$ , and quintuplet  $\Pi_u$  states, correlating to the first dissociation limit  $\text{Se}(^3\text{P}) + \text{Se}(^3\text{P})$ . The PECs of electronic states relate to the predissociation of the  $B^3\Sigma_u^-$  state are presented in Fig. 2 along with the 21 lowest discrete vibrational levels of the  $B$  state. Since the repulsive and semi-bound states are all correlated to the first dissociation limit while the  $B^3\Sigma_u^-$  state is correlated to the higher  $\text{Se}(^3\text{P}) + \text{Se}(^1\text{D})$  asymptote, the predissociation type is Hertzberg Ic, it implies that the crossings between repulsive states lead to predissociation of the  $B$  state into the  $\text{Se}(^3\text{P}) + \text{Se}(^3\text{P})$  limit, the overlap between the vibrational levels of the  $B$  state and the dissociation continuum is the main predissociation mechanism. The classical crossing point of the  $B^3\Sigma_u^-$  state and repulsive  $^1\Pi_u$  is located between  $\nu = 5$  and  $\nu = 6$  vibrational levels of the  $B^3\Sigma_u^-$  state, it agrees with the experimental observation by Katô *et al.*<sup>[20]</sup> in which the strong predissociation occurs at  $\nu = 5$  levels of the  $B$  state. The second observed predissociation for  $\nu = 13 \sim 15$  of the  $B$  state is due to the crossing with

the  $^5\Pi_u$  state, as shown in Fig. 2, while the calculated crossing point is located at a higher level ( $\nu = 17$ ) of the  $B$  state because the spin mixed level splitting is not considered in calculations.

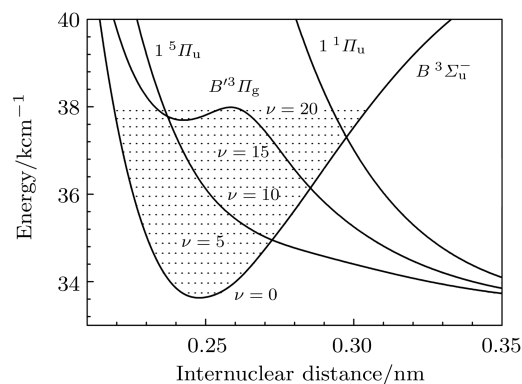


**Fig. 2.** The PECs for predissociation of the  $B^3\Sigma_u^-$  state.

The spin-orbit coupling matrix elements were calculated to support the above classical point of view on the predissociation mechanism of the  $B^3\Sigma_u^-$  state. Since the spin-orbit interaction between  $B^3\Sigma_u^-$  and  $^3\Pi_g$  is forbidden by parity selection rules, Table 3 only collects the  $\langle ^1\Pi_u | H_{so} | ^3\Sigma_u^- \rangle$  and  $\langle ^5\Pi_u | H_{so} | ^3\Sigma_u^- \rangle$  matrix elements at different internuclear distances.

When spin-orbit interaction is introduced, only  $\Omega$  becomes the so-called ‘good quantum number’ to represent the spin-mixed electronic states. The matrix elements  $\langle {}^1\Pi_u(\Omega=1)|H_{so}|{}^3\Sigma_u^-(g\Omega=1)\rangle$  ranging from  $248\text{ cm}^{-1}$  to  $283\text{ cm}^{-1}$  at the bond distance of  $2.6\text{ \AA}\sim 2.9\text{ \AA}$ , indicate that the  $\Omega=1$  PEC of  $B^3\Sigma_u^-$  state ( $B1_u$ ) diabatically joins into the lower dissociation limit along PEC of  ${}^1\Pi_u$  state, which corresponds to the first predissociation experimentally observed for at  $\nu=4\sim 6$  levels of the  $B$  state. The relative large values of spin-orbit matrix elements  $\langle {}^5\Pi_u|H_{so}|B^3\Sigma_u^- \rangle$  for both  $\Omega=0$  and  $\Omega=1$  are found at different bond distances in Table 3, which indicates that the  $B^3\Sigma_u^-$  state is perturbed near high levels ( $\nu=17$ ) by the quintet  $\Pi_u$  state via spin-orbit interaction. As discussed above, the repulsive singlet and quintet  $\Pi_u$  are both responsible for the predissociation of the  $B^3\Sigma_u^-$  state occurring at  $\nu=5$  and  $\nu=17$  vibrational levels. The present quantum theoretical result agrees reasonably with the Katô’s experiments where the predissociation of the  $B^3\Sigma_u^-$  state at  $\nu=4\sim 6$  and  $\nu=13\sim 15$  were observed.<sup>[20]</sup>

**Table 3.** Absolute values of spin-orbit matrix elements in  $\text{cm}^{-1}$  at different internuclear distances.

$R/\text{\AA}$	2.60	2.70	2.80	2.90
$\langle {}^1\Pi_u(\Omega=1) H_{so} {}^3\Sigma_u^-(\Omega=1)\rangle$	248	263	275	283
$\langle {}^5\Pi_u(\Omega=0) H_{so} {}^3\Sigma_u^-(\Omega=0)\rangle$	257	265	261	255
$\langle {}^5\Pi_u(\Omega=1) H_{so} {}^3\Sigma_u^-(\Omega=1)\rangle$	445	459	452	442

### 3.3. Lifetime of the $B^3\Sigma_u^-$ state

The valence  $p_x$  and  $p_y$  electrons in  $\pi_g$  orbit give rise to strong vertical transition  $B^3\Sigma_u^- - X^3\Sigma_g^-$ . The electric dipole transition moments as functions of bond distances were calculated using the ic-MRCI (SD) method with the nonrelativistic all-electron and RECP basis set and are illustrated in Fig. 3, along with the calculated results, including scalar relativistic effects from Ref. [14]. The transition moments has a maximum at  $\sim 1.9\text{ \AA}$ , while it decreases rapidly out of the Franck-Condon region. The behaviour of the transition moment function is due to the spin-forbidden transition  ${}^1D-{}^3P$  of Se at the dissociation atom limits. In Fig. 3, the two all-electron calculated transition moments agree very well, while the calculated RECP transition moments are about 15% lower than the AE

values regardless of whether or not the scalar relativistic effects are included in AE calculations. The difference is caused by the change in inner-shell electron wavefunctions for different molecule geometries, while in the RECP molecular orbital calculations the inner-shell electrons are treated using fitted constant effective potentials from atomic multi-configuration Dirac-Fock wavefunctions and the change in inner-shell potential is neglected. As shown in Fig. 3, the difference in transition moment between AE and RECP calculations becomes smaller at longer bond length; this is because the molecule at a longer bond distance is closer to the atom limits where the RECP is accurately fitted. The AE calculated transition moment function is used to evaluate the lifetimes of the  $B$  state in the present work.

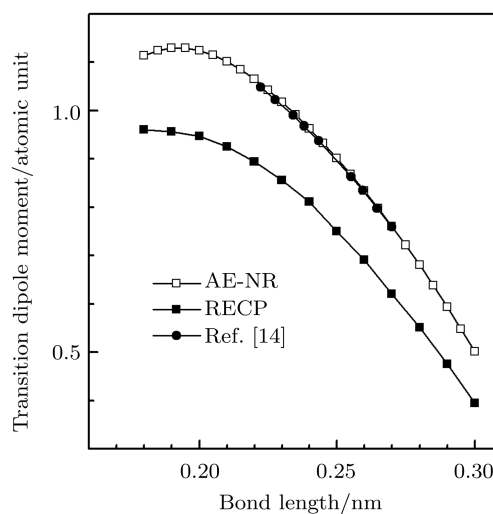


**Fig. 3.** Transition dipole moment (in atomic unit) of the  $B-X$  transition of  $\text{Se}_2$  molecule as functions of the internuclear distance. Open square: all-electron nonrelativistic (AE-NR) results; solid square: results by using relativistic effective core potential (RECP) basis; solid circle: scalar relativistic calculation from Ref. [14].

The Einstein coefficients  $A_{v',v''}$  of spontaneous transitions from  $B^3\Sigma_u^-$  ( $v'=0\sim 6$ ) to  $X^3\Sigma_g^-$  ( $v''=0\sim 99$ ) were then evaluated using the calculated transition moment function and PECs according to the formula (2). Because of the deep potential width of the ground state  $X^3\Sigma_g^-$ , a large number of lower levels ( $v''=0\sim 99$ ) is used for convergence. Detailed calculations show that  $v'-0$  transitions are weak. For instance, in  $3-v''$  transitions, the  $3-5$  transition is the strongest one due to the relative large bond length difference ( $\sim 0.3\text{ \AA}$ ) between  $X$  and  $B$  states, and the vertical transition is not the strongest one.

The lifetimes of vibrational levels of  $B$  states were then calculated using formula (2), as shown in Fig. 3 along with the available experimental results for comparison. The calculated lifetimes of  $v' = 0 \sim 6$  vibrational levels for the  $B$  state are 49.3(52.0), 49.5(52.6), 49.8(52.8), 50.0(53.1), 50.3(53.5), 50.7(54.4), 51.0(54.6) ns, respectively, by the AE(RECP) basis set, excluding or including scalar relativistic effects. The small difference ( $\sim 6\%$ ) between the nonrelativistic and relativistic results is probably due to the partial cancellation of scalar relativistic contributions for  $B$  and  $X$  states. In Fig. 4, the lifetime value of  $v' = 0$  approximate is located at the middle of two early  $v$ -independent experimental results. The lifetimes of  $v' = 3 \sim 6$  by the ic-MRCI method with the AE and RECP basis set are all close to the upper limits of the latest experimental values, or fall into the error bars of experimental results for AE values of  $v' = 4, 6$  levels. The experimental lifetimes give a turning point at  $v' = 5$ , while the present theoretical lifetime function is monotonically increasing, this minor difference arises from the perturbation of the  ${}^1\Pi_u$  state via spin-orbit interaction, as discussed in Subsection 3.2. The transition from  $B^3\Sigma_u^- (\Omega = 1)$  to  ${}^1\Pi_u (\Omega = 1)$  at  $v' = 5$  decreases the lifetimes of the  $B$  state, while for other vibrational levels of the  $B$  state, the large relative energy differences make this transition less important. The RECP values are systematically larger than experimental ones with  $\sim 10\%$  error due to the overestimated relative energies, as discussed in Subsection 3.1. According to the spin-orbit constant and relative energy listed in Table 1, if spin-orbit coupling is introduced, the calculated lifetimes will be  $< 5\%$  shortened and closer to experimental observations. As a brief conclusion, the present level of theory gives satisfactory calculated results of radiative lifetimes for the relative heavy elements system  $\text{Se}_2$ , and may be extended to other molecular system. Further studies of PECs and transition properties, including both scalar relativistic effects and spin-orbit interaction utilizing states interaction technique with all

spin-free states coupled together, are now in progress.

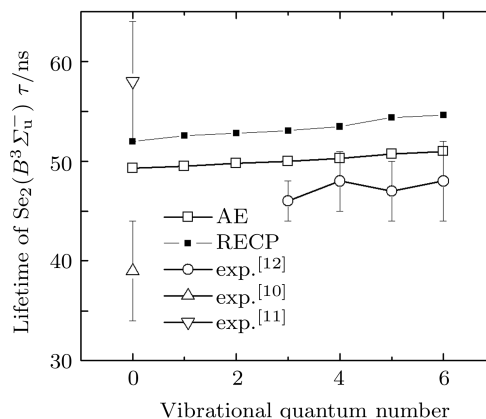


Fig. 4. Calculated lifetimes of  $B^3\Sigma_u^-$  ( $v' = 0 \sim 6$ ) levels by the AE (open square) and RECP (solid square) basis sets.

## 4. Summary

The twelve low-lying spin-free electronic states of the  $\text{Se}_2$  molecule have been investigated by the internal-contracted multireference configuration interaction method with the all-electron basis set and relativistic effective core potential. The potential energy curves and transition moment functions of the  $B^3\Sigma_u^- - X^3\Sigma_g^-$  transition were calculated, the spectroscopic constants of bound states were fitted and compared with experiments; the predissociation mechanism of the  $B^3\Sigma_u^-$  state was discussed based on spin-orbit *ab initio* calculations, the coupling with  ${}^1\Pi_u$  and  ${}^5\Pi_u$  leads to the predissociation of the  $B^3\Sigma_u^-$  state according to the present theoretical results. The lifetimes of  $B^3\Sigma_u^-$  ( $\nu = 0 \sim 6$ ) were calculated with the all-electron basis set and relativistic effective core potential plus its valence basis set, respectively. The results reasonably agree with the available experiments.

## Acknowledgement

We acknowledge the High Performance Computing Center (HPCC) of Jilin University for supercomputer time.

## References

- [1] Leone P R and Kosnik K G 1977 *Appl. Phys. Lett.* **30** 346
- [2] Wheeler M D, Newman S M and Orr-Ewing A J 1998 *J. Chem. Phys.* **22** 1998
- [3] Kiljunen T, Eloranta J and Kunttu H 2000 *J. Chem. Phys.* **17** 2000
- [4] Yan B, Pan S F, Wang Z G and Yu J H 2005 *Acta Phys. Sin.* **54** 5618 (in Chinese)
- [5] Gibson N D, Kortshagen U and Lawler J E 1996 *J. Appl.*

- Phys.* **79** 7523
- [6] Herzberg G (translated by Wang D C) 1983 *Molecular Spectra and Molecular Structure I: Spectra of Diatomic Molecular* (Beijing: Science Press) p. 462 (in Chinese)
- [7] Prosser S J, Barrow R F, Effantin C, Incan J and Verges 1982 *J. Phys. B* **15** 4151
- [8] Setzer K D, Dorn A, Lorenz and Fink E H 2003 *J. Mol. Spectr.* **221** 13
- [9] Heaven M, Miller T A, English J H and Bondybey V E 1982 *Chem. Phys. Lett.* **91** 251
- [10] Stolyarov A, Kuzmenko N E, Harya Y A and Ferber R S 1989 *J. Mol. Spectr.* **137** 251
- [11] Gouedard G and Lehmann 1975 *Comput. Rend. Acad. Sci. (Paris)* **280** B471
- [12] Martinez E, Basterrechea F J, Puyuelo P and Castano F 1995 *Chem. Phys. Lett.* **236** 83
- [13] Bhanuprakash K, Hirsch G and Buenker R J 1991 *Mol. Phys.* **72** 1185
- [14] Heinemann C, Koch W, Linder G, Reinen D and Widmark P 1996 *Phys. Rev. A* **54** 1979
- [15] Yan B, Pan S F and Guo Q Q 2008 *Chin. Phys. B* **17** 3318
- [16] Yan B and Feng W 2010 *Chin. Phys. B* **19** 033303
- [17] Balabanov N B and Peterson K A 2005 *J. Chem. Phys.* **123** 064107
- [18] Peterson K A, Figgen D, Goll E, Stoll H and Dolg M 2003 *J. Chem. Phys.* **119** 11113
- [19] Werner H J, Knowles P J, Lindh R, Manby F R, Schütz M and others *MOLPRO* version 2006.1, a package of *ab initio* programs, see <http://www.molpro.net>
- [20] Katô Hajime and Baba Masaaki 1995 *Chem. Rev.* **95** 2311